Ultra high precision surface structuring by synchronizing a galvo scanner with an ultra short pulsed laser system in MOPA arrangement

B. Jaeggi*[a], B. Neuenschwander[a], U. Hunziker[a], J. Zuercher[a], T. Meier[b], M. Zimmermann[b],
K. H. Selbmann[c], G. Hennig[d]

[a]Bern University of Applied Sciences, Institute for Applied Laser ,Photonics and Surface Technologies, Pestalozzistrasse 20, CH-3400 Burgdorf, Switzerland

[b]Bern University of Applied Sciences, Institute for Mechatronic Systems, Pestalozzistrasse 20, CH-3400 Burgdorf, Switzerland

[c]Bern University of Applied Sciences, Institute for Printing Technologies, Pestalozzistrasse 20, CH-3400 Burgdorf, Switzerland

[d]Daetwyler Graphics, Flugplatz, CH-3368 Bleienbach, Switzerland

ABSTRACT

For surface and 3D structuring the ultra short pulsed laser systems are mostly used in combination with galvo scanners. This work reports on the synchronization of the scanner mirror motion with the clock of the laser pulses, which is usually in the range of 100 kHz and higher, by a modification of the electronic scanner control. This synchronization facilitates the placement of the small ablation craters from single pulses with the precision of about 1 µm relative to each other. The precise control of the crater positions offers the possibility to test and optimize new structuring strategies. Results of this optimization process with respect to minimum surface roughness, steepness of wall, accuracy to shape and efficiency will be presented.

Keywords: Ultra short pulsed laser system, galvo scanner, synchronization, surface roughness, steepness of wall, efficiency

1. INTRODUCTION

A standard process for surface structuring applications is the filling of a given outline with a parallel hatching. Commonly 3D structures are built up in a series of slices by adapting the outline and the hatch angle from slice to slice. The lines of the hatch pattern are generated with mechanical axes, usually galvo scanners, and the laser pulse train is switched on and off via an external modulator which is gated by a signal from the axes control software. Figure 1 shows what can happen in this situation. If the pulse train is switched on with the start of the axes acceleration the distance from pulse to pulse (pitch) increases until the axes has reached its final speed (figure 1a). Such lines show deep marks at the start and ending points of the single lines but the effective position of these points are well defined. To avoid the phenomenon of deep marking a so called sky-writing option can be used. Sky-writing means that the axes already have the correct velocity at the beginning of the marking. With sky-writing option a displacement of the start position of plus/minus the distance between two consecutive pulses has to be accepted (figure 1b). Therefore for high precision structuring applications this combination suffers from inaccuracies due to the asynchronous motion of the axes relative to the pulse train. If this problem should be avoided it will be necessary to synchronize the axes motion onto the output pulse train of the laser system or vice versa (figure 1c). In the case of a Q-switched laser system the pulse train can be shifted by the external control software. This is a simple solution and is e.g. supported by many scanner control software. Currently in industrial applications ultra short pulsed laser systems will be used if high requirements concerning accuracy, defined surface roughness and small heat affected zone are demanded. Unfortunately with Q-switched laser system the achievable pulse durations are not short enough for precise micro-processing.

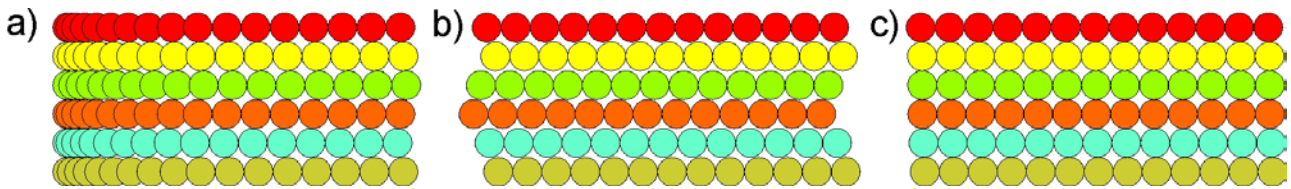*beat.jaeggi@bfh.ch; phone +41 (0)34 426 41 93; fax +41 (0)34 423 15 13

Figure 1: Start positions of the different strategies: a) standard setup without sky-writing option; b) standard setup with the sky-writing option; c) synchronized system

The today available industrially suited ultra short pulsed systems are turnkey systems, set up in a master oscillator power amplifier (MOPA) arrangement with a passively mode locked seed laser, followed by a pulse picker and a rod or disk amplifier to prepare the output pulse train. However, a MOPA design has at the beginning of the amplifier chain a passively mode locked seed laser. Also the value of the pulse repetition rate can be chosen it is a risky task to shift the pulse train with the first pulse picker located directly after the seed oscillator. Risky because a change in the time interval between two consecutive pulses leads to a variation of the energy of the first or the first few pulses, known as first pulse problem. Finally one has to tune the gating module and the followed mechanical components on the laser pulse train.

2. SYNCHRONIZATION

The standard laboratory setup includes control software and a controller board that controls the scan head and the POD-module, as seen in figure 2.

The movements of the scanner are written into an instruction list on the controller board with the control software. The instruction list is then executed according to a software or hardware trigger. Depending on the type of movement the controller enables the POD.
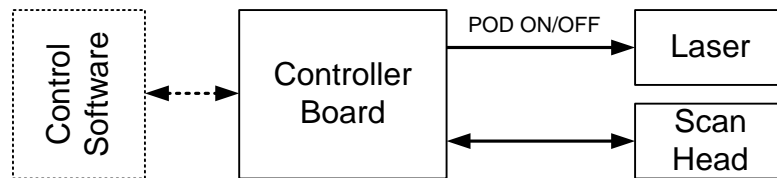

Figure 2: Standard Laboratory Setup

As mentioned above it is not possible to modify the phase of the laser frequency. Therefore the scanner's movements have to be synchronized with the laser pulses. Figure 3 shows the structure developed to synchronize the scanner movements with the laser pulses.
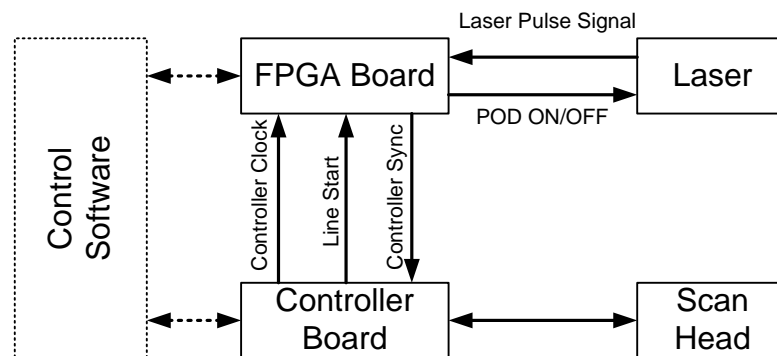

Figure 3: Synchronized Setup

Since the execution of the commands in the instruction list is depending on the controller clock, which can be modified with the controller sync entry, it is possible to lock the phase of the controller clock to the laser pulse signal. The phase detector and the filter of this phase locked loop were implemented in a Field Programmable Gate Array (FPGA) and the controller sync signal is generated by a controlled oscillator.

In order to create three dimensional structures black-and-white images are provided to the control software. The images are divided into lines and transmitted to the FPGA. Accordingly a linear movement is included into the instruction list. The start of the scanner movement is communicated to the FPGA and the laser pulses is enabled (white parts of the image) or not (black parts of the image).

3. EXPERIMENTAL SETUP

As a source for the laser pulses a DUETTO (Time Bandwidth Products) generating 10 ps pulses at 1064 nm wavelength was used. Afterwards the pulses were converted to a wavelength of 532 nm by Second Harmonic Generation. The repetition rate is ranging from 50 kHz to 1 MHz. Due to the cycle time of the POD-module, the usable repetition rates are in a range from 50 to 300 kHz. The energy per pulse is up to 200 µJ. The used scanner system was an IntelliScan 14 of Scanlab. The laser beam was circular polarized using a λ/4-plate and directed through 4 mirrors and a variable beam expander onto the galvo scanner. With a 100 mm telecentric f-theta objective the beam was focused to a spot radius w_0 of 5.7 µm, which was measured with a slit scanning beam profiler. Additionally a beam quality $M^2 \leq 1.1$ was measured, and therefore a Gaussian shaped beam could be assumed. All experiments were performed with the target surface in the focal plane of the telecentric f-theta objective. The analyzed sample material was copper Cu-DHP (in US: C12 200) whose surface was polished with a diamond suspension. The structures were measured by using a laser scanning microscope, a light optical microscope and a scanning electron microscope. To determine the achieved surface roughness and the taper angle, squares with a side length of 1 mm were ablated. To present the limits of the system concerning minimum ablated structures, bars and pillars with different side length were ablated. To compare the achieved results, structures with the asynchronous system were ablated, as well. In this case the scanner movements were controlled by the Laserdesk-software of Scanlab.

4. THEORETICAL BACKGROUND AND LASERPARAMETERS

4.1 Theory

For high precision micro machining the material parameters are important. As a consequence of the two-temperature-model which is discussed in the literature[1-5], the logarithmic ablation law between the peak laser fluence in the beam centre F_0 of the laser pulse and the ablation depth z_{abl} is given by[5-12]:

$$z_{abl} = \delta \cdot \ln\left(\frac{F_0}{F_{th}}\right) \tag{1}$$

The ablation depth z_{abl} depends on the two material parameters penetration depth δ and threshold fluence F_{th}. The threshold fluence F_{th} describes the minimum energy which is needed to ablate material. The penetration depth δ is the ability of the energy to penetrate into the material. With equation 1, and assuming a Gaussian beam shape, the ablated volume per pulse for a Gaussian beam is given by[9-12]:

$$\Delta V = \frac{1}{4} \cdot \pi \cdot \delta \cdot w_0^2 \cdot \ln^2\left(\frac{F_0}{F_{th}}\right) \tag{2}$$

As shown in the literature[7-10, 12], the volume ablation rate can be maximized by choosing the optimum repetition rate at a given average power. From the expression for the optimum repetition rate and the maximum volume ablation rate one can show that under best condition the ablated volume per pulse ΔV reads for a Gaussian beam and a top hat beam as well:

$$\Delta V = \pi \cdot w_0^2 \cdot \delta \tag{3}$$

With equalizing the equations 2 and 3, and using the fluence of the laser pulse in function of the pulse energy:

$$F_0 = \frac{2 \cdot E_p}{\pi \cdot w_0^2} \tag{4}$$

The optimum pulse energy E_p is:

$$E_p = \frac{\pi \cdot w_0^2}{2} \cdot F_{th} \cdot e^2 \tag{5}$$

By a given repetition rate f_{rep}, the average power P_{av} is:

$$P_{av} = E_p \cdot f_{rep} \tag{6}$$

With the threshold fluence of 0.11 J/cm^2 and the penetration depth of 6.67 nm, which are determined for 512 pulses in an ablation study, the optimum pulse energy is 0.4 µJ. For a repetition rate of 100 kHz and 300 kHz the average power is 40 mW and 120 mW, respectively.

5. RESULTS AND DISCUSSION

5.1 Scan Strategies

As a first task the best scan strategy for ablating structures with a good result concerning the surface roughness and the optical effect was investigated. To compare the surface roughness the arithmetical mean roughness Ra was measured with the laser scanning microscope. The optical effect achieves the best value if no periodical structures appear. Due to the limitation of the synchronization software, it is possible to mark lines only in one direction. Scanning diagonal lines is not possible at the moment, and is subject of running investigations.
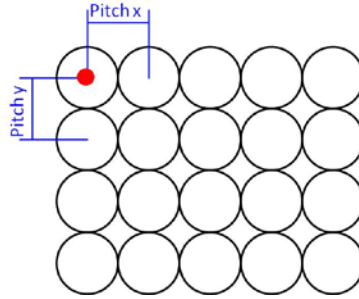

Figure 4: Layer with the start position (red dot) and the pitches in x- and y-direction

To find the best strategy, squares with a side length of 1 mm and a constant number of layers were ablated. The design of the layer was always the same. I. e., a given pitch which is the distance between two consecutive spots in both directions and a given starting point (red point in figure 4). The first strategy was 120 layers, and 4 defined start positions. Each start position was addressed 30 times in the same sequence (1 to 4). The pitch was about 3 µm. Due to the multiple crossing of each position, periodical structures at the bottom of the structure could be observed. The second strategy was 120 layers as well, but with 120 different start positions, determined randomly with a uniformed distribution with the lower and upper endpoint of 0 and half of the pitch. The Ra-value decreases, because every layer starts with another start position and so the same position is addressed only once. But a periodical pattern at the bottom of the structure rest. The periodical pattern disappeared at the same surface roughness when the uniformed random distribution of the start positions was changed to a normal or Gaussian distribution with the mean parameter μ of 0 and the standard deviation σ of a quarter pitch. Additional strategies with different arrangements of the pulses were tested. But always a periodical structure was observed. The best strategy found to be a normal or Gaussian random distribution of the start positions.

5.2 Surface roughness

The laser parameters were given by equation 5 and 6. The used average power was 40 mW by a repetition rate of 100 kHz. To find the optimal distance between two consecutive pulses (pitch in x- and y-direction) tests with different distances from 1/8 - 2·w_0 what conform to 0.75 µm to 12 µm, were done. With changing the distance, the whole absorbed energy changes when the number of layers is constant. Therefore the number of layers for a constant energy during the whole process has to be adjusted. That means for a pitch of 1 µm, the number of layers was 13, for 3 µm

120 layers and for a pitch of 12 µm 1920 layers. By using the Laserdesk software hatched squares were ablated with different numbers of layers and different hatch distances. Between two consecutive layers the hatch was turned around an angle of 15°.
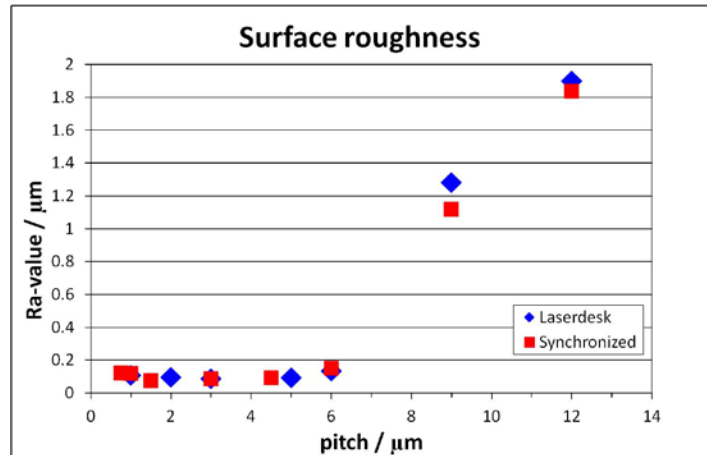

Figure 5: A comparison of the achieved *Ra*-values versus the pitch

The lowest obtained surface roughness amounts about 90 nm for a pitch of about half of the spot radius. The minimum *Ra*-values of the synchronized structures (red dots in figure 5) were in the same range as the values of the structures controlled with the Laserdesk software (blue points in figure 5). In the region with a pitch of a half spot radius the surface roughness is nearly constant. With an increasing pitch, the overlap between two consecutive pulses disappeared, and the surface roughness increases as well.

5.3 Steepness of wall

In the cross section view (figure 6a) the definition of the taper angle is shown. The taper angle was measured at the same squares as the surface roughness. With the asynchronous system two different options can be chosen. With the sky-writing option (green dots in figure 6b) the bottom close to the boundary of the structure has the same deepness as the rest of the structure (see figure 7b). But the taper angle is even more flat cause of the different start positions of the lines showed in figure 1b. Without the sky-writing option (red dots in figure 6b), the taper angle increase, but deep marks on the ground can be observed (see figure 7a), cause of the acceleration. The increasing of the angle can be explained as followed: Due to the acceleration the pitch between two consecutive pulses is small. Therefore no big deviation of the start position appears. In the case of the sky-writing option, the deviation of the start position is plus/minus one pulse that means plus/minus the pitch, what equates a range of 6 µm. So the taper angle is lower (green dots in figure 6b) but no acceleration marks appear (see figure 7b). The synchronized system is a compromise of these two strategies. The taper angle is maximized to the values without the sky-writing (blue dots in figure 6b) and no acceleration marks occur, see figure 7c.
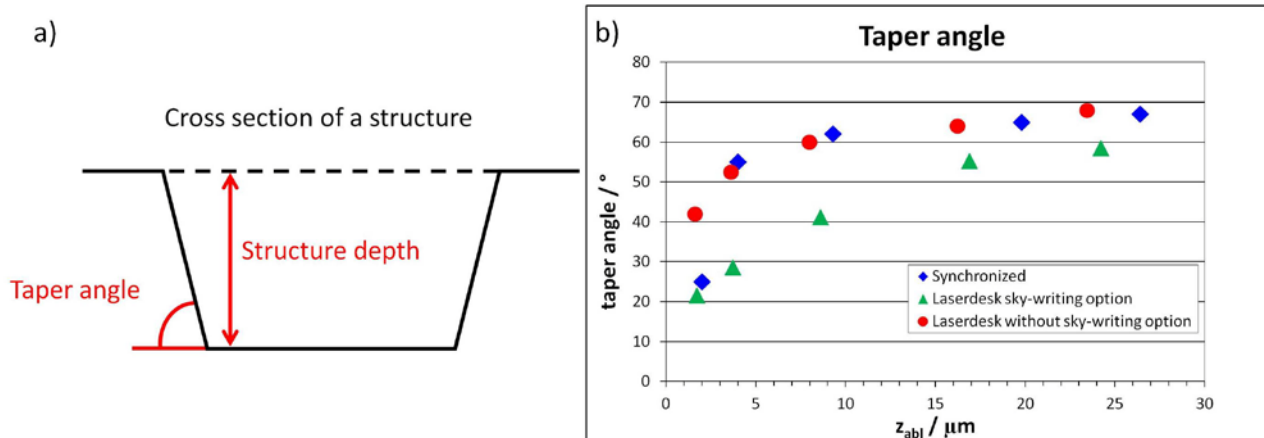
Figure 6: a) Cross section of a structure; b) the taper angle versus the structure depth on the right side
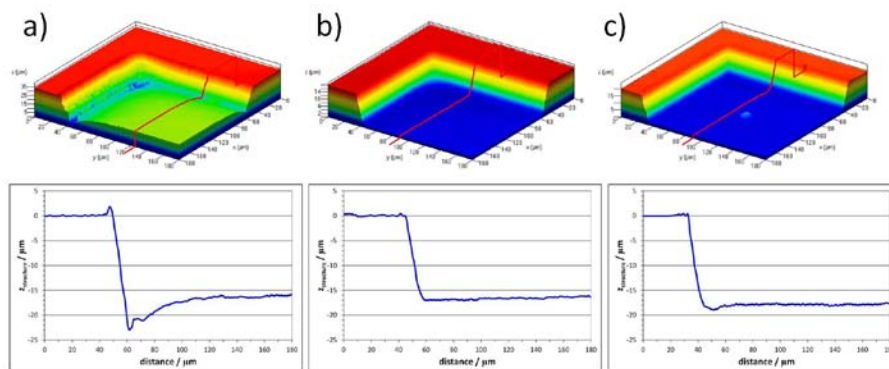

Figure 7: Taper angle of a) Laserdesk software without sky-writing; b) Laserdesk software with sky-writing; c) Synchronized system; performed with 120 mW, 300 kHz, 3 µm pitch, 120 layers

5.4 Minimum structures

For testing the minimal ablated structures a repetition rate of 300 kHz and an average power of 120 mW were chosen. The structures were performed with a pitch of 3 µm and 60 layers. Two different structures were examined: bars and pillars with a square horizontal projection. The minimal structure should still full fill the following two conditions: firstly the height of the structure should be leveled with the surface. Secondly the horizontal projection in the case of the pillars should be squared. The minimum side length was always measured at the top of the structure. For the minimal bars we used a black-and-white bitmap with a pitch of 1 µm, but only every third pixel was shot. This strategy only works for 1-dimensional structures like the bars but not for pillars. To find the minimum structure dimension, bars with different web widths from 5 to 19 µm were produced. To compare the minimum bars with the Laserdesk software rectangles with a given distance between each rectangle were ablated. The hatched rectangles are built up of 60 layers and between two consecutive layers the hatch angle was turned around angle of 3°. With the increasing of the distance between two rectangles from 1 µm to 30 µm the minimum bar can be estimated. In figure 8a the minimal bars are shown for the process with the Laserdesk software without the sky-writing option on the left side. Figure 8b shows the bars performed with the sky-writing option. The bar in the middle of this image achieves the condition for a minimum structure, defined at the beginning of this section. Figure 8c shows the structures produced with the synchronized system. Also the bar in the middle reaches the condition for a minimum structure. The minimum web width for the synchronized system and the asynchronous shows values in the range of 3 to 5 µm, measured at the top of the structure. This corresponds to a minimum web width in the range between a half and one spot radius. The advantage of the synchronized system is the higher taper angle. Figure 8d shows the periodical structure with the minimum bars performed with the synchronized system to show reproducibility.
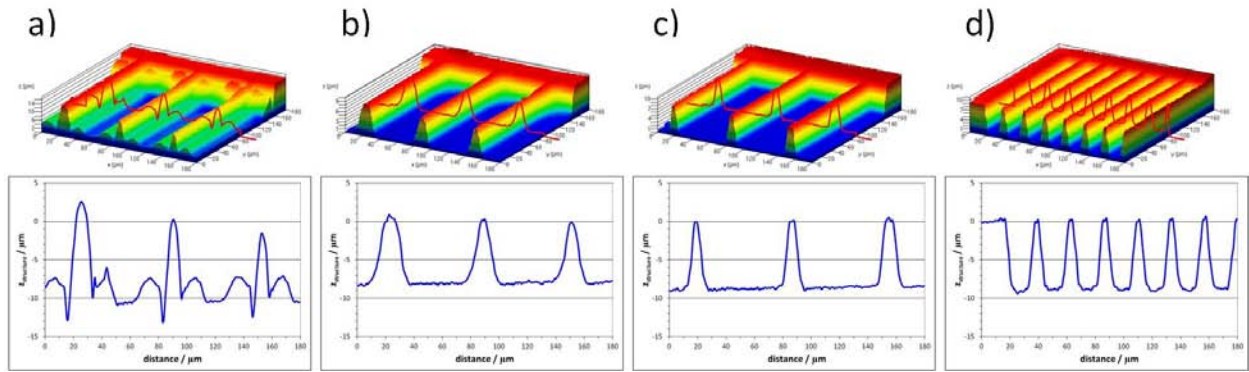
Figure 8: Minimum bars controlled by a) Laserdesk without sky-writing; b) Laserdesk with sky-writing; c) synchronized system; d) periodical minimum bars; 120 mW, 300 kHz, 1 µm pitch, 60 layers

For the minimal pillars a black-and-white bitmap was created using a matlab routine. One Pixel equates one laser pulse. The structures were performed with a pitch of 3 µm and 60 layers. With the Laserdesk software the given outline of the pillars was filled with a hatch. The hatch distance was 3 µm and between two consecutive layers the hatch was turned around an angle of 3°. With increasing the side length of a pillar from 3 to 21 µm the minimum pillar can be estimated. In figure 9a the minimum pillars for the Laserdesk software without the sky-writing mode are shown. There the typical marks due to the acceleration of the scanner mirrors are clearly seen. The figure 9b shows the pillars produced with the sky-writing mode and figure 9c shows the pillars from the synchronized system. The minimum side length of the squared horizontal projection, measured at the top of the structure was for both strategies in a range about 6 µm, which is more or less the spot radius.
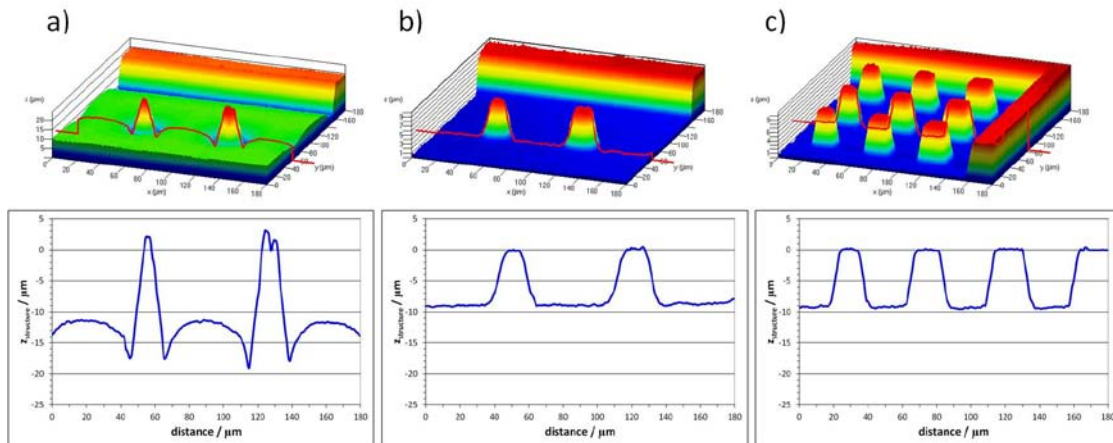

Figure 9: Minimum pillars, controlled by a) Laserdesk without sky-writing; b) Laserdesk with sky-writing; c) synchronized system, 120 mW, 300 kHz, 3 µm pitch, 60 layers

5.5 Bitmaps

The synchronization software needs a black-and-white bitmap file. The bird, which is shown in figure 10, was ablated from a black-and-white image. It shows a comparison between a microscope image and the SEM image. In this experiment once the positive and once the negative form were ablated. In figure 11 some other examples for ablating black-and-white images are shown. On the left hand side always the microscope image and on the right hand side the original image are shown. If a grayscale image will be used, different black-and-white layers have to be used by using a grayscale threshold for the different layers. By the transformation of a grayscale image in a 3D-image we have to consider the ablation depth. Black parts of the grayscale image should be the deepest points of the 3D-image. In figure 12 we can see the original grayscale picture (figure 12a), a typically black-and-white layer (figure 12b) and at last the ablated image (figure 12c) which is produced with 300 kHz and 120 mW and a pitch of 3 µm. The number of different layers was 100. By working with 3D-data, the data have to be compiled in black-and-white layers by using a threshold

value for the height. Figure 13b shows as an example the topography of Switzerland, based on the real 3D-data. This image was occurred by ablating 447 different layers.
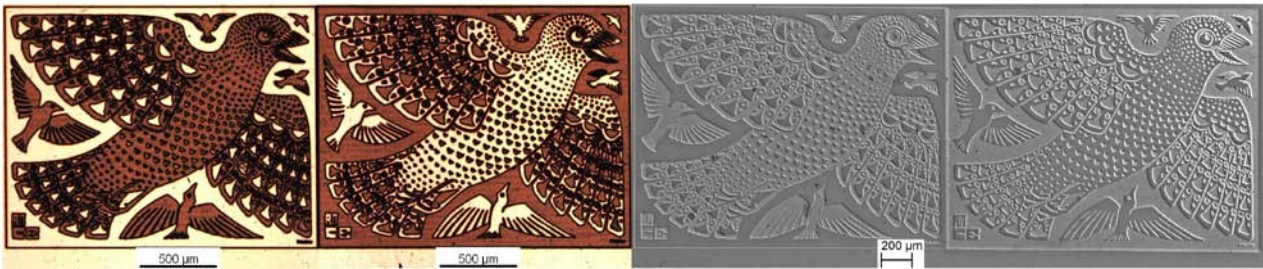

Figure 10: Comparison of the microscope image with the SEM image, 120 mW, 300 kHz, 3 µm pitch, 30 layers[14]

Figure 11: Structures based on black-and-white images: comparison of the original picture and the microscope image, 120 mW, 300 kHz, 3 µm pitch, 30 layers[15, 16, 17]
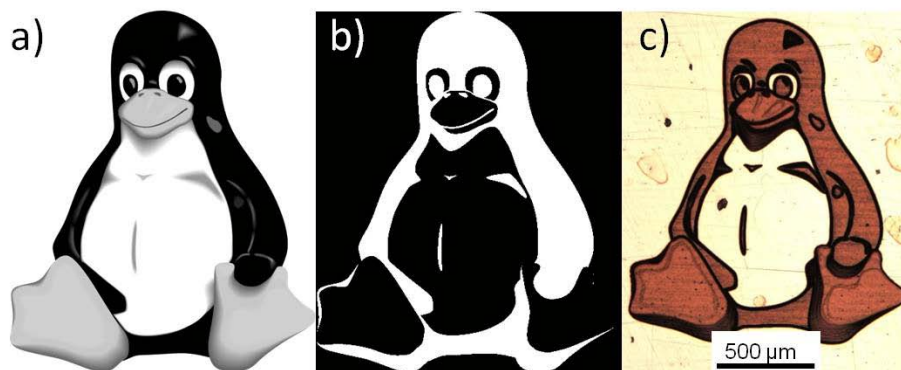

Figure 12: Structure based on a grayscale image: a) original grayscale image[18]; b) typical black-and-white layer; c) microscope picture of the structure; performed with 120 mW, 300 kHz, 3 µm pitch, 100 layers
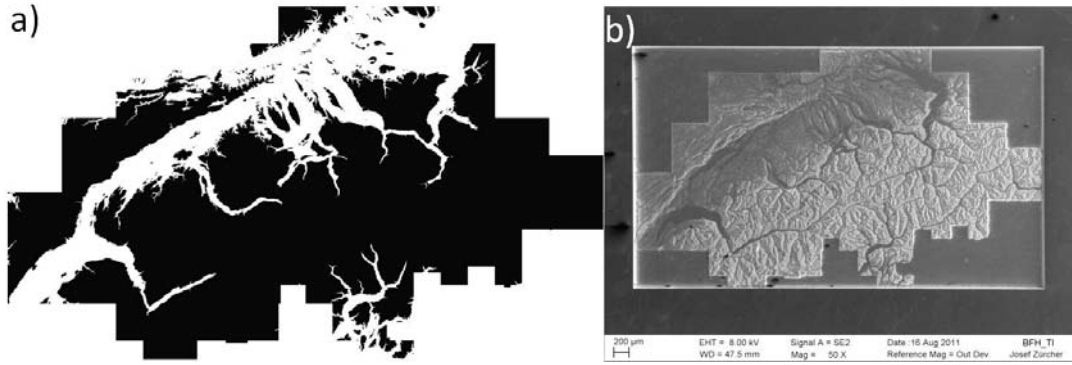
Figure 13: Structure based on topography data of Switzerland[19] a) typical black-and-white layer; b) SEM image of the structure, 120 mW, 300 kHz, 3 µm pitch, 447 layers

With the used laser system and the Laserdesk software it was not possible to generate bitmaps. The software generates a signal with a different voltage value for the different grayscale values. With this signal the laser output power can be changed. For our laser system only the laser on/off signal to control the POD-module is used, as seen in figure 2. The laser output power cannot be adjusted during the process. Therefore a comparison is not possible.

5.6 Periodical surface structuring

With the synchronized system it is possible to arrange the craters with a given distance between each other. During one layer one pulse per cavity appears. In figure 14a we see a pattern with 100 pulses per cavity. The average power was 120 mW at a repetition rate of 300 kHz. The used pitch was 1 µm. In the normal asynchronous system the scanner moves to the first cavity, ablates the crater and moves then to the next position. With the synchronized system, the used bitmap has been scanned, and always when a white pixel appeared, a laser pulse was released. By using 100 layers the bitmap has been scanned 100 times. At the end at every white pixel a cavity occurs. With the synchronized system the ablation of the cavities is much more efficient, cause the acceleration before and after the ablation of one crater falls away. In figure 15 another pattern with a detail view is shown. It is clearly seen that all pulses strikes at the same point with a high accuracy concerning the position, during the movement of the synchronized scanner. Other strategies are to ablate hexagonal combs or cubes, which are based on a hexagonal structure, seen in figure 14b, c. The combs and cubes are performed with a pitch of 3 µm, an average power of 120 mW, a repetition rate of 300 kHz and 30 layers.
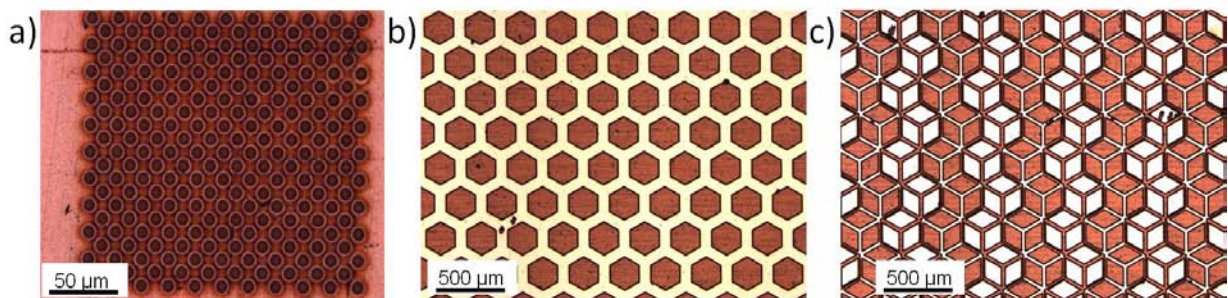

Figure 14: Periodical surface structuring: a) cavity pattern; b) comb pattern; c) cube pattern based on a hexagonal structure
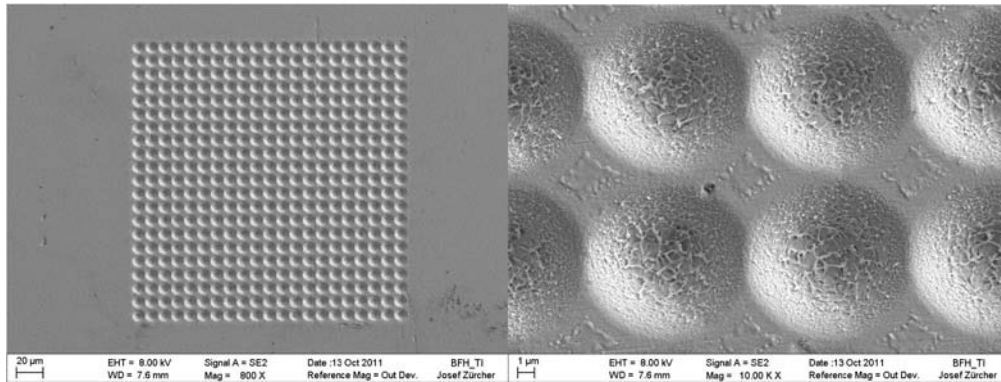
Figure 15: SEM images of a cavity pattern with a detail view, 120 mW, 300 kHz, 100 layers

6. SUMMARY AND OUTLOOK

If we compare the synchronized system with the asynchronous scanner, the achieved *Ra*-value is in the same range of about 90 nm by a pitch of about a half spot radius. The taper angle increases with increasing depth of the structure for all tested strategies. By ablating structures, controlled by the Laserdesk software, either deep marks at the bottom and a high taper angle appears without the sky-writing option, or the taper angle is flat but no marks appears if the sky-writing option is used. By using the synchronized system, the advantages of both strategies can be combined. That means no marks at the bottom of the structure near the boundary and a high taper angle. The minimum structures are in both cases, controlled by the Laserdesk software and using the synchronized system, are in the range of a half and one spot radius measured at the top of the structure. By structuring a periodical surface due to ablate craters the efficiency is much higher, due to the continuous motion of the scanner mirror. During the experiments the limited factor was the repetition rate due to the cycle time of the used POD-module. With a new gating-module the limited factor will be the mark speed of the scanner system, and no longer the repetition rate. So the cycle time will decrease. With a further development of the software, also new strategies can be tested. But the main task, the synchronization of mechanical components, in our case a galvo scanner, on the laser clock is done, and it shows advantages compared with the asynchronous motion of the scanner mirrors. For faster micro machining, new beam control system should be tested to achieve higher marking speeds, because the scanner system reaches his limits. With the faster movement, the higher repetition rates of the laser system could be used. The precision is limited due to the optical system. This problem can avoid by using an axicon as a focusing lense and high precision axes which is reported in Michalowski et al[13].

7. ACKNOWLEDGEMENT

REFERENCES

[1] S. Nolte, "Mikromaterialbearbeitung mit ultrakurzen Laserpulsen", Dissertation, Duvillier Verlag, Göttingen,

[2] S. Nolte, C. Momma, H. Jacobs, A. Tünnermann, B.N. Chichkov, B. Wellegehausen et al., "Ablation of metals by ultrashort laser pulses", J. Opt. Soc. Am. B / Vol 14, No. 10 / October 1997

[3] C. Körner, "Theoretische Untersuchungen zur Wechselwirkung von ultrakurzen Laserpulsen mit Metallen", Dissertation der technischen Fakultät der Universität Erlangen-Nürnberg, 1997

[4] B.N. Chichkov, C. Momma, S. Nolte, F. von Alvensleben, A. Tünnermann, "Femtosecond, picosecond and nanosecond laser ablation of solids", Appl. Phys. A 63 (1996) 109-115

[5] C. Momma, S. Nolte, B.N. Chichkov, F. v. Alvenleben, A. Tünnermann: Precise laser ablation with ultrashort pulses, Appl. Phys. Sci. 109/110 (1997) 15-19

[6] C. Momma, B.N. Chichkov, S. Nolte, F. von Alvensleben, A. Tünnermann, H. Welling et al., "Short-pulse laser ablation of solid targets", Opt. Commun. 129 (1996) 134-142

[7] B. Jaeggi, B. Neuenschwander, M. Schmid, M. Muralt, J. Zuercher and U. Hunziker, "Influence of the Pulse Duration in the ps-Regime on the Ablation Efficiency of Metals", Physics Procedia 12 (2011) 164-171

[8] M. Schmid, B. Neuenschwander, V. Romano, B. Jaeggi and U. Hunziker, "Processing of metals with ps-laser pulses in the range between 10ps and 100ps", Proc. of SPIE, Vol. 7920, paper 792009, (2011)

[9] B. Neuenschwander, B. Jaeggi, M. Schmid, U. Hunziker, B. Luescher, C. Nocera, "Processing of industrially relevant non metals with laser pulses in the range between 10 ps and 50 ps", Paper M103, ICALEO 2011

[10] B. Neuenschwander, G. Bucher, G. Hennig, C. Nussbaum, B. Joss, M. Muralt, S. Zehnder et al., "Processing of dielectric materials and metals with ps laserpulses", Paper M101, ICALEO 2010

[11] G. Raciukaitis, M. Brikas, P. Gecys, B. Voisiat, M. Gedvilas, "Use of High Repetition Rate and High Power Lasers in Microfabrication: How to keep Efficiency High? ", JLMN Journal of Laser Micro/Nanoengineering; Vol. 4 (3) p186-191 (2009)

[12] B. Neuenschwander, G. Bucher, C. Nussbaum, B. Joss, M. Muralt, U. Hunziker et al., "Processing of dielectric materials and metals with ps-laserpulses: results, strategies limitations and needs", Proceedings of SPIE vol. 7584 (2010)

[13] A. Michalowski, C. Freitag, R. Weber and T. Graf, "Laser surface structuring with long depth of focus", Proc. SPIE, Vol. 7920, paper 79200W (2011)

[14] http://www.wikipaintings.org/en/m-c-escher/birds

[15] http://britton.disted.camosun.bc.ca/jbtess97.htm

[16] http://www.zazzle.ch/rosen_lithographie_fotoskulptur-153582013095294502

[17] http://wandtattoos.solineo.ch/shop/index.php?popup_box=images&pID=90020&products_id=90020&page=2

[18] http://en.wikipedia.org/wiki/File:Tux.svg

[19] Bundesamt für Landestopographie swisstopo